Non-linearity issues in the dynamic compact model generation

Marta Rencz*, Vladimir Székely**
*MicReD Ltd, Hungary
**Budapest University of Technology and Economics, Hungary
rencz@micred.com

Abstract

The dynamic compact thermal R_{th}-C_{th} *(RC)* models of packages generated from the transient measurements or simulations are usually temperature independent, that is linear. This is theoretically erroneous. In this paper we show how to generate nonlinear compact thermal models. Algorithms with which network simulators can simulate nonlinear R_{th} and C_{th} elements are also given. With the help of the generated correct nonlinear models of packages we present various experiments, in which the order of magnitude of the error, caused by neglecting the temperature dependence of the R_{th} and C_{th} elements of the dynamic compact thermal models is checked.

Keywords

Compact thermal models, dynamic compact models, nonlinear models, R_{th} and C_{th} models

1. Introduction

The transient or dynamic compact thermal R_{th}-C_{th} models of packages, represented usually by electrical *RC* elements, are practically always considered to be temperature independent, that is linear. These models are used to describe the thermal behavior of the modeled packages or subsystems in a broad temperature range, where the assumption of linearity is theoretically erroneous. Since the temperature dependence of the thermal conductivity of the materials used in the packages is pronounced [1] [2] one may presume that neglecting the temperature dependence of these models results in non-negligible errors, especially for large temperature excursions. In practice however, the temperature dependence of the transient compact models of packages, is never considered, see e.g. some of the important papers in the subject, as [3], [4] or [5].

The main reason for this negligence probably is, that the usual network simulators, with which these models are finally simulated are not prepared to simulate circuits with nonlinear circuit elements. The nonlinear thermal R_{th}-C_{th} models can be exercised only with simulators that are prepared to simulate the behavior of temperature dependent, that is, $R_{th}(T)$ and $C_{th}(T)$ models. So that, in order to verify the behavior of the nonlinear models, first we had to realize temperature dependent $R_{th}(T)$ and $C_{th}(T)$ models, and build them into a circuit simulator program. After this we could start to develop nonlinear package models, in order to compare their behavior to the behavior of linear models.

The present work is the continuation of the work introduced at the Therminic workshop [6]. In our work we intended to check the order of magnitude of the error caused by neglecting the temperature dependence of the R_{th} and C_{th} elements of the dynamic compact thermal models.

In the first part of this paper we summarize the sources of non-linearity in the thermal behavior of electronic packages. After this we present a methodology for the creation of temperature dependent, that is non-linear dynamic compact models, in which all the model elements may be temperature dependent. The presented methodology is general, applicable for most of the usual structures to generate temperature dependent compact models either from simulation or from measurements. In *Section 4* we give an algorithm for the realization of temperature dependent $R_{th}(T)$ and $C_{th}(T)$ elements in circuit simulators. With the application of all of these we can accomplish simulation experiments for the comparison of the linear and non-linear dynamic compact models of the examined package, finally we evaluate the results.

2. The sources of non-linearity in the thermal behaviour of packages

There are two main sources for the nonlinearities in the dynamic package models. The most important source is the pronounced temperature dependence of the thermal material parameters, the thermal conductivity and the volumetric heat capacity values. If the compact models are calculated from the measured thermal behavior we encounter a further source of the nonlinearity, coming from the nonlinearity of the applied temperature sensors during the measurements. In the present paper we do not discuss this latter one.

2.1. The temperature dependence of thermal material parameters

The main source of the thermal non-linearity is the temperature dependence of the λ thermal conductivity of the matter. Different materials behave differently: pure metals show very little temperature dependence of λ, see Fig. 1. It is interesting to note that the thermal conductivity of some metallic alloys e.g. brass, grows with the temperature. Semiconductors are usually characterized by a rapidly diminishing thermal conductivity with increasing temperature, see Fig. 2. Some ceramics, as the Al_2O_3 or BeO behave similarly to the semiconductors, see Fig. 2.

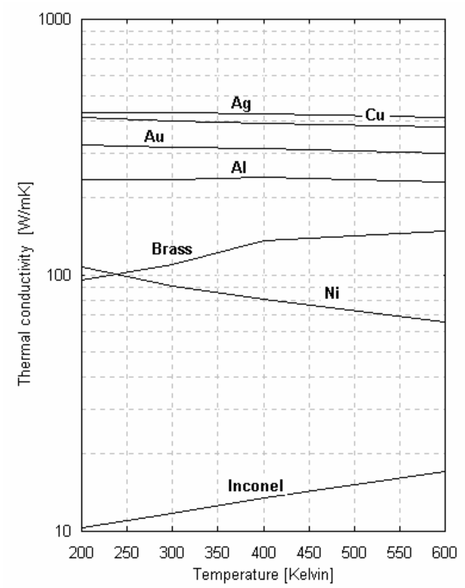

Fig. 1 Thermal conductivity of pure metals and metallic alloys [1]

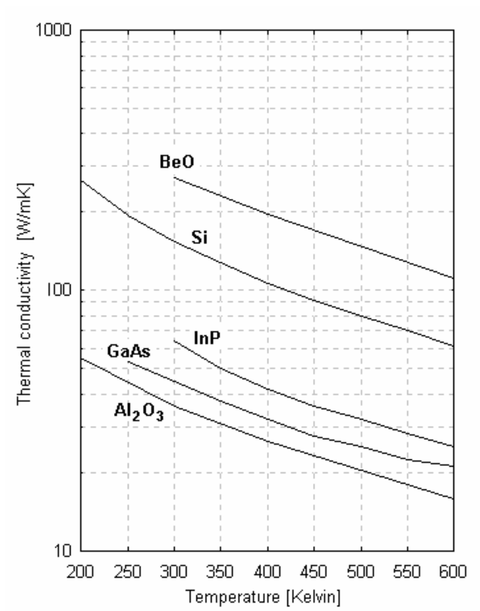

Fig. 2 Thermal conductivity of semiconductors and ceramics [1],[2]

Although the temperature dependence of the λ thermal conductivity of different materials can follow different functions approximate common descriptions are possible. A frequently used model is the description with an exponential function, as:

$$\lambda = \lambda_0 \exp(\alpha_\lambda (T - T_0)), \qquad (1)$$

where λ_0 is the value of the thermal conductivity at the reference temperature $T_{0,}$ and α_λ is the coefficient of temperature dependence (CTD) of λ. It is useful to know that this α_λ value is equal to the relative change of λ for 1^{o}C temperature rise. The α_λ values for some common materials of packages are presented in Table 1., calculated from the data of [1].

Table 1.

Material	λ_0 W/mK	α_λ 1/K	c_{v0} Ws/m^{3}K	α_c. 1/K
Cu	401	-0.0001	$3.44 \cdot 10^6$	0.0003
Ni	90.7	-0.00012	$3.95 \cdot 10^6$	0.0008
Ag	429	-0.000094	$2.47 \cdot 10^6$	0.00017
Inconel	11.7	0.0014	$3.74 \cdot 10^6$	0.00075
Al_2O_3	36	-0.0031	$3.04 \cdot 10^6$	0.002
Si	148	-0.004	$1.66 \cdot 10^6$	0.001

T_0 = 300 K

α values are averages for the 300-400K range

In the dynamic behavior the temperature dependence of the heat capacitances may also play a role. Fortunately this effect is rather small and often negligible in the 0-150^{o}C range. For the description of the temperature dependence of the heat capacity a function similar to Eq.(1) can be used as :

$$c_v = c_{v0} \exp(\alpha_c (T - T_0)), \qquad (2)$$

where c_v is the volumetric heat capacity, c_{vo} is its value at $T_{o,}$ and α_c is the coefficient of its temperature dependence. The temperature dependence of c_v for a few materials is plotted in Fig. 3 Values of c_{v0} and α_c are presented also in Table 1.

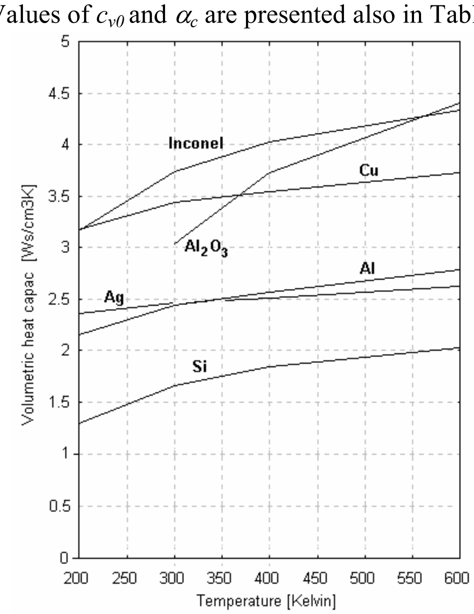

Fig. 3 Volumetric heat capacity data [1]

As it is visible from Fig. 3 the temperature dependence of c_v in the most interesting 300-450K range is small, compared to that of λ.

3. A method for creating non-linear dynamic compact models

The methodology that we are presenting is fairly general. It applicable for most shapes of circuit models or any way or methodology of generating the compact models, and it is usable, either simulation or measurement is the source of information about the time dependent thermal behavior of the package.

3.1. The idea

To create temperature dependent compact models we have to

1. create compact models on different temperatures, with fixed network topology
2. find the relationship between the corresponding element values and the temperature, and
3. Consider these temperature dependent R_{th} and C_{th} element values in the temperature dependent model. [6]

In order to create dynamic compact models on different temperatures we have to accomplish transient measurements or simulations with small temperature excursions, in temperature intervals where the thermal conductivity values may be considered constant. The appropriateness of this procedure will be shown in *Section 5*. The dynamic compact models of the packages have to be created by any of the usual methodologies for each of these temperatures. These measurements or simulations have to be repeated on gradually increasing temperatures, and the corresponding compact models determined for all the measurements. With the help of curve fitting the temperature dependence of each element value may be determined, obtaining this way the correct dynamic compact models, where all the elements are temperature dependent.

3.2. Experimental verification: generation of a non-linear model

Following this idea we have created the non-linear model of a power package from measured thermal transients, and in order to collect information about the temperature dependence of package models we have accomplished various measurement and simulation experiments.

In our first experiment the heating curves, that is the step response functions of the same packaged power transistor structure were measured with small temperature rise, while the ambient temperature was changed gradually from 10^{o}C to 80^{o}C. During the thermal transient measurements the temperature rise was limited in 20^{o}C, assuring the linearity of the individual measurements. The resulting cumulative structure functions [4] are plotted in Fig. 4. On these curves the thermal capacitance of the structure is plotted in the function of the thermal resistance, measured from the junction (x=0) towards the ambient (x→∝), in the direction of the main heat flow path. Consequently, the total thermal resistance of the structure is the R_{th} value, when C_{th}→∝. It is well observable that, according to the expectations, the overall thermal resistance of the structure increases with the ambient temperature.

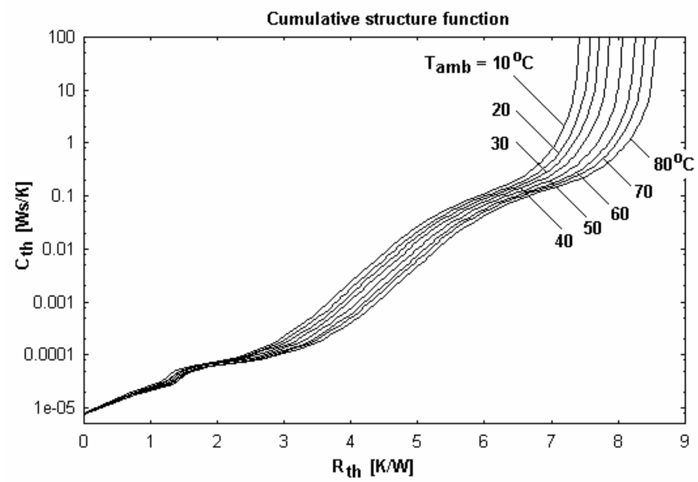

Fig. 4 Cumulative structure functions calculated on different ambient temperatures, with small temperature excursions

If the heat flow path of the structure consists of different materials, as it is the case normally with IC packages, then the different regions of the heat-flow path show different temperature dependence, since the different materials in the path have different thermal coefficients for the thermal conductivity. Constructing an appropriate lumped model of the heat-flow path we can follow these differences.

The cross section of the measured structure, shown in Fig. 5 consists of 4 different main materials in the heat flow path from the die to the ambience. Consequently, if we wish to determine the individual temperature dependencies of the various layers we should construct a 4 resistor – 4 capacitor equivalent circuit. The equivalent circuits are generated with the help of the THERMODEL program [8]. The generated ladder type circuits on two different temperatures are shown in Fig.6.

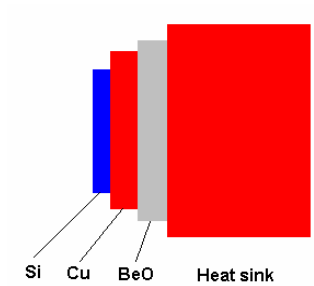

Fig. 5 The cross section of the measured structure

Fig. 6 shows the 4-stage model circuit on two different temperatures and in Fig. 7 we provide the individual thermal resistance and capacitance values for the 8 generated models.

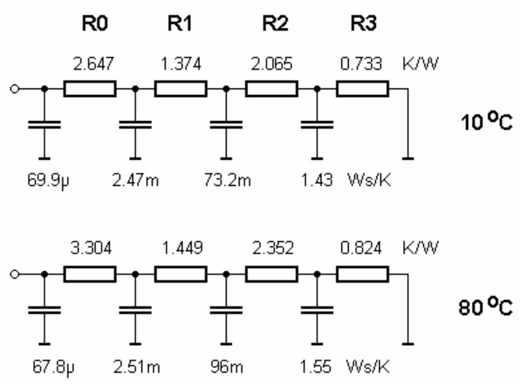

Fig. 6 The 4 stage RC ladders, generated on different temperatures

Observing that the thermal capacitance values are far less temperature dependent in this package than the thermal resistance values we consider in this model the C_{th} values independent of temperature.

It is well observable that the thermal resistance values show now very different temperature dependence. The relatively high R0 and R2 thermal resistances corresponding to the silicon and the ceramics depend strongly on the temperature, while the smaller R1 and R3 thermal resistances are almost independent of the temperature.

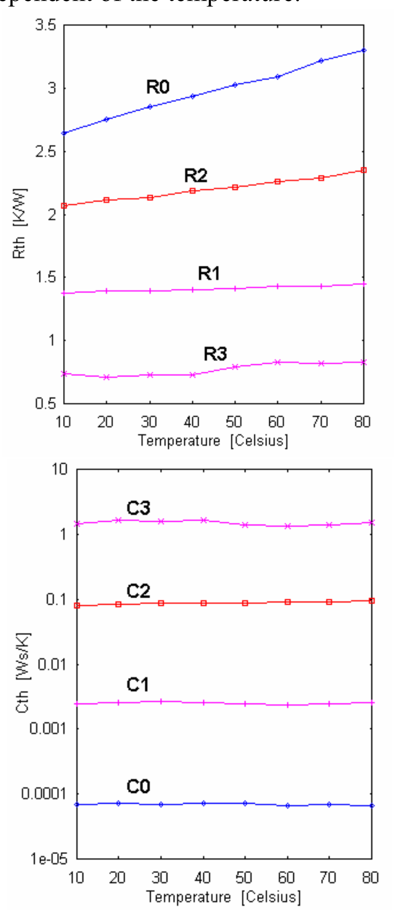

Fig. 7 The temperature dependence of the thermal resistance and capacitance values in the structure of Fig. 5, calculated from measured transient curves [9]

It is worth to check the thermal coefficients of the different regions. The $\alpha_{Rth} = 1/R_{th} \times dR_{th}/dT$ values are constructed from the structure functions and are shown in Fig. 8 for the various regions of the heat flow path. (Since $R_{th} \sim 1/\lambda$, $\alpha_{Rth} = -\alpha_{\lambda}$.), see [6]. If we compare these values with the structure of Fig. 5, we find good agreement for the averaged temperature coefficients of the different regions with the appropriate reference book values of Table 1, shown with numerical values in the figure.

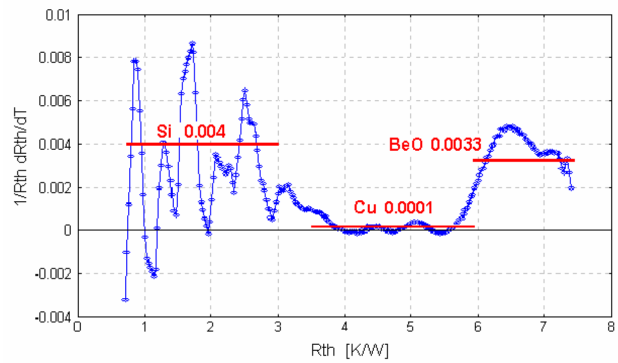

Fig. 8 The α_{Rth} temperature coefficients in the various parts of the heat flow path, see also Fig. 5

From these series of measurements, namely from the curves of Fig. 7 we can determine the temperature dependence of the individual thermal resistance values of the compact models. Considering these values in the compact model we have created a correct non-linear temperature dependent compact model of the examined package. This model is shown in Fig. 9.

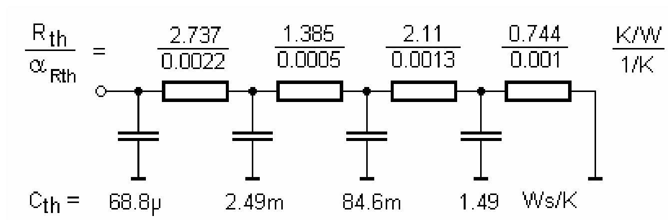

Fig. 9 The correct non-linear RC model of the structure of Fig. 5

According to Fig. 7 the temperature dependence of the thermal resistance values in this particular case might be even easily approximated by linear functions, making the modeling very simple, but we will calculate with the more general temperature dependence of Eq.(1).

If each resistance is taken into account by the value that corresponds to *its expected average temperature*, then we have a linear RC ladder model representing a rougher approximation of the thermal behavior.

4. Temperature dependent R_{th} and C_{th} models for network simulators

To check the error caused by neglecting the temperature dependence of the element values in the compact models of packages we should exercise both the linear and the non-linear models with the same input signals and check the differences in the resulting heating curves. The problem is however, that circuit simulator programs are not capable to calculate with non-linear resistors.

To overcome this problem we have built a non-linear thermal resistance model into the TRANS-TRAN electro-thermal network simulator program [10].

4.1. Nonlinear R_{th} model for circuit simulators

This non-linear thermal resistance model uses the topology shown in Fig. 10. For the calculation of the temperature dependence Eq.(1) is used, where the *T* actual temperature is the average of the two node temperatures of *T1* and *T*2.

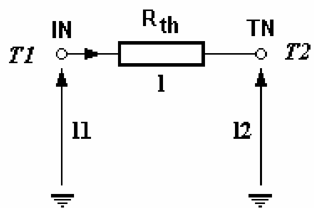

Fig. 10 Model topology of the nonlinear thermal resistance

The applied model equation is as follows:

$$R_{th}(T) = R_{tho}\exp(\alpha_{Rth}(T - T_0)), \qquad (3)$$

The simplified C language source code of the model is shown in Fig. 11, where. `vbr[]` are the branch voltages/temperatures, `brcu[]` are the currents/heat-currents of the branches, and `t00` is the ambient temperature.

4.2. Nonlinear C_{th} model for circuit simulators

The non-linear heat capacitances can be modeled similarly to the modeling of the temperature dependent thermal resistances in a network simulator. The modeling is now even simpler, since only one branch is needed to represent a non-linear heat capacitance, as it is connected always between a 'NODE' and the thermal "ground".

The actual heat capacitance value is calculated in our case by the expression of Eq. (4).

$$C_{th}(T) = C_{tho}\exp(\alpha_{Cth}(T - T_0)), \qquad (4)$$

During the solution the capacitance value is fed to the `cbr[]` array of branch capacitances, updated after each time step during the transient solution (time integration).

The simplified C language source code of the model of a nonlinear thermal capacitor is presented in Fig. 12.

```
/*****************************************@*/
int thresnl(int l)                       @@*/
/* Function:                              @*/
/* The nonlinear Rth model of TR-TR       @*/
/* Rth=value*exp(tempcoef*((T1+T2)/2-Tref)) @*/
/*****************************************@*/
/*      B R A N C H E S         ATTRIBUTES @*/
/* l  thermal resistance IN--->TN  value    @*/
/* l1 temperature branch GND-->IN tempcoef  @*/
/* l2 temperature branch GND-->TN           @*/
/*****************************************@*/
{ double rth0,rth,gth,tempcoef,p,s,t1,t2;
  int l1,l2;

  l2=1+(l1=1+l);
  rth0=attri[n2l[l]].val;
  tempcoef=attri[n2l[l]+1].val;

  t1=-vbr[l1]+t00;
  t2=-vbr[l2]+t00;

  rth=rth0*exp(tempcoef*(0.5*(t1+t2)-25.0));
  gth=1.0/rth;
  brcu[l]=p=(t1-t2)*gth;

  s=0.5*p*tempcoef;
  gtrload(-(gth-s));          /* dP/dvbr[l1] */
  gtrload(gth+s);             /* dP/dvbr[l2] */
  return(0);
}
```

Fig. 11 Simplified C language source code of the non-linear Rth model

```
/*****************************************@*/
int thcapnl(int l)                       @@*/
/* Function:                              @*/
/* The nonlinear Cth model of TR-TR       @*/
/* Cth=value*exp(tempcoef*(T-Tref))       @*/
/*****************************************@*/
/*      B R A N C H E S         ATTRIBUTES @*/
/* l  heat capacitance NODE-->GND  value    @*/
/*                                tempcoef  @*/
/*****************************************@*/
{ double cth0,cth,tempcoef,temp;

  cth0=attri[n2l[l]].val;
  tempcoef=attri[n2l[l]+1].val;

  temp=vbr[l]+t00;

  cth=cth0*exp(tempcoef*(temp-25.0));
  cbr[l]=cth;
  return(0);
}
```

Fig. 12 Simplified C language source code of the non-linear C_{th} model

The presented $R_{th}(T)$, $C_{th}(T)$ modeling method is a very good approximation for such types of models where the model topology reflects the physical structure. In other words: when each thermal resistance of the model corresponds to a more or less well defined region of the package. The reason of having to set this condition is, that in our nonlinear modeling approach the R_{th} actual value of the non-linear thermal model-resistor is determined by its own temperature. This means that the model resistors have to hold (approximately) the same temperature as their physical counterparts. The same is true for heat capacitances.

Consequently, we may state that, in case of e.g. the star-shape type models like the examples of Fig. 13 and Fig. 14, or the one-port Cauer ladder models, like the model of Fig. 9 the used $R_{th}(T)$and $C_{th}(T)$ models provide the real actual values of the modeled material regions. In case of other model structures, like the impedance matrix modeling approach, or certain model elements of the DELPHI type models, where the average of the terminal temperatures of a given element can not be considered to be a good approximation of the real temperature of the actual model element, this $R_{th}(T)$, $C_{th}(T)$ modeling approach has to be used with great care.

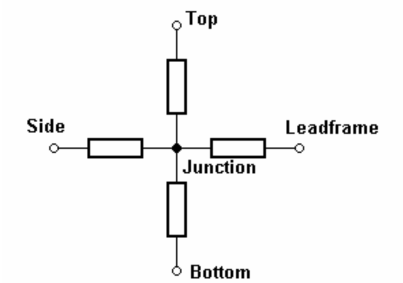

Fig. 13 DC Model topology, appropriate to be simulated with the presented method

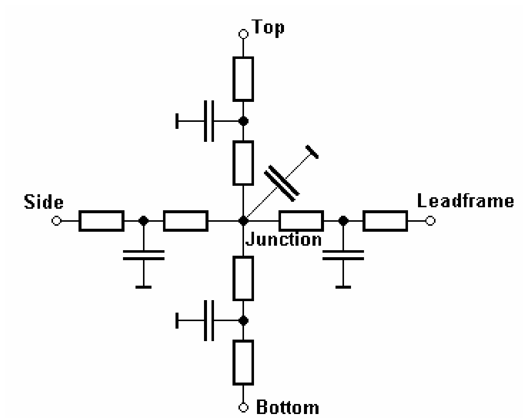

Fig. 14 Dynamic model topology, appropriate to be simulated with the presented method.

Having a network simulator with a temperature dependent thermal resistance as standard element in the model set we could easily perform further simulation experiments.

Part of the TRANS-TRAN netlist, describing the chain of Fig. 9 is shown in Fig. 15. Here `THRES_NL` is the identifier of the nonlinear thermal resistance. This element has two attributes: the thermal resistance value at 25 °C and the temperature coefficient.

```
R0:THRES_NL(X0,X1)=2.737,0.0022;
C0:THCAP(X0,GND)=68.8e-6;
R1:THRES_NL(X1,X2)=1.385,0.0005;
C1:THCAP(X1,GND)=2.49e-3;
R2:THRES_NL(X2,X3)=2.11,0.0013;
C2:THCAP(X2,GND)=0.0846;
R3:THRES_NL(X3,GND)=0.744,0.001;
C3:THCAP(X3,GND)=1.49;
```

Fig. 15 Part of the TRANS-TRAN netlist, describing the chain of Fig. 9

With the help of this nonlinear network model, the behavior of the linear and nonlinear models can be compared in various circumstances.

5. Comparison of the results simulated with linear and nonlinear models of the same structure

We have applied a large power step input on the $R_{th}(T)C_{th}$ model, where the temperature dependence was modeled according to Fig. 9. This results in a large temperature increase. We compared the calculated heating curves to the ones calculated with the models containing no temperature dependence, but considering the average R_{th} values from Fig. 7. The two curves are presented in Fig. 16.

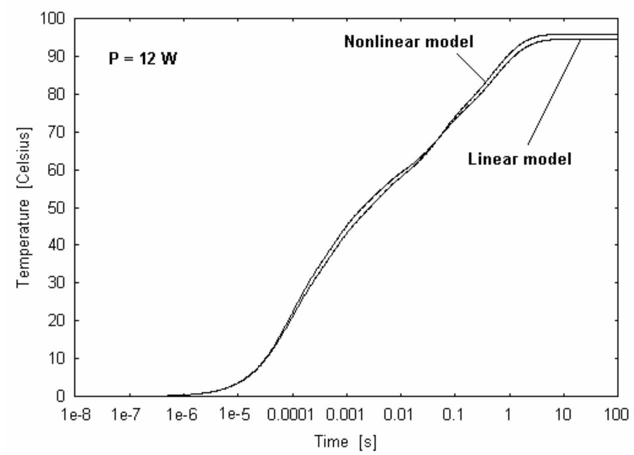

Fig. 16 Comparison of the calculated heating curves. The figure shows that the linear model was created for the operation at 65°C

As it is visible from this figure the difference between the curves calculated with and without the consideration of the correct temperature dependence of the R_{th}-values in the model circuit is negligible. The maximal difference of the 2 curves is less than about 3% in the whole temperature range, and the average difference is even less than about 1%.

5.1. Thermal transients calculated with nonlinear models

With the help of the TRANS-TRAN program a simulation experiment was carried out. The thermal behavior of the structure of Fig. 17 was simulated. The 4 layer Si-Cu-Al_2O_3-Al structure models the main heat flow path of a chip in a package: the strongly and lightly temperature dependent layers are alternating in about 1:1 ratio. The individual layers are modelled with 2 and 4 stage RC ladders. The transient behaviour was simulated with different excitations at different ambient temperatures.

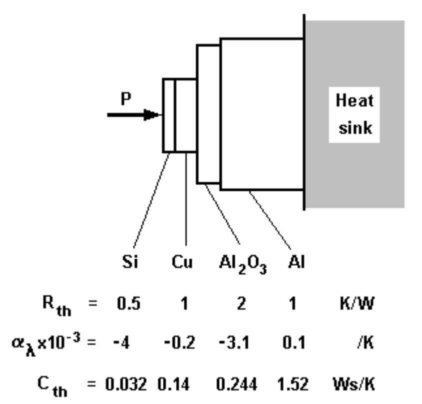

Fig. 17 The simulated structure

In Fig. 18 heating curves are presented obtained at T=25 ^{o}C ambient temperature with different dissipation values, but for the sake of the better comparability normalised to the 1W dissipation. The real dissipation and maximal temperature rise values are though shown at each curve.

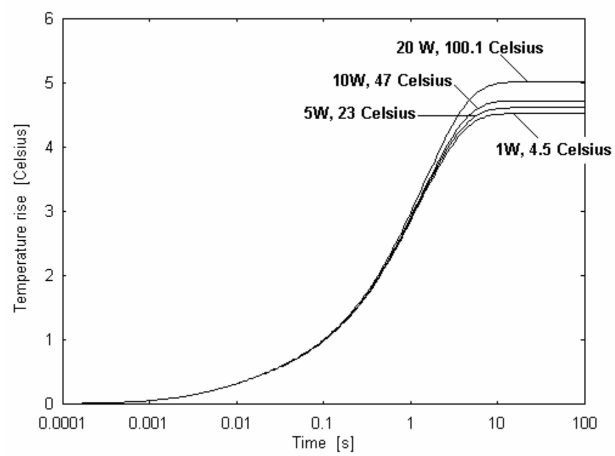

Fig. 18 Heating curves normalised for 1W power at Tamb=25°C

We can suppose that nonlinear effects do not play role in case of the 1 W dissipations, since the temperature rise is only 4.5°C. Note, that the curve of the 5W dissipation, resulting in 23^{o}C temperature rise is hardly different from this curve, their maximal difference is 2,2 %. The error is even in the case of 47 °C temperature rise under 4.5%, but in case of the 20W dissipation, that is, resulting in 100°C temperature rise the error starts to increase sharply. We can draw the conclusion, that a powering resulting in not higher than 25 °C temperature rise does not cause significant non-linear effects.

In the next simulation experiment the effect of the ambient temperature on R_{th} was examined. Each curve of Fig. 19 was calculated with 1W powering, resulting in about 5°C temperature rise, consequently the non-linear effects may be neglected.

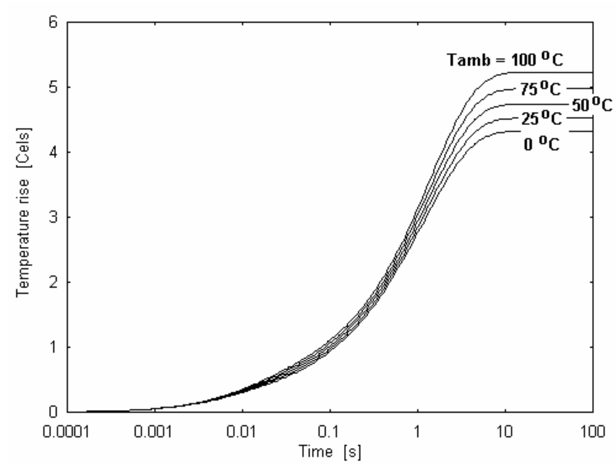

Fig. 19 Heating curves at different ambient temperatures for 1W powering

As we can see from this figure the nonlinearities result in an about 20% difference between the curves at 0 and 100°C.

6. Conclusions

We have presented a way to generate correct temperature dependent dynamic compact models for the characterization of the thermal behavior of packages. With the help of this methodology we have created the temperature dependent compact model of a power package. We have found that the obtained thermal capacitance values are practically temperature independent, the thermal resistance values show characteristically different, but linear temperature dependence. From the temperature dependence of the individual R_{th} values we could even get back the textbook thermal coefficients of the thermal conductivity values of the materials used in the package.

We have created an electrical model to simulate the behavior of the temperature dependent dynamic compact $R_{th}(T)C_{th}$ model, and compared the simulated results with the simulation results obtained by the temperature independent $R_{th}C_{th}$ model.

We have found, that the error committed by using temperature independent models is in the order of magnitude of 0-4%, if the temperature rise does not exceed ~50°C.

We may state from obtained and presented results, that the use of linear RC dynamic compact thermal models is usually not resulting in considerable errors in the calculation of the dynamic thermal behavior of packages. For higher temperature rise (>80-100 ^{0}C), however, the use of non-linear compact models is recommended.

Since most of the temperature dependence of the usual packages is attributed to the temperature dependence of the silicon and the ceramics, as it is also visible in Fig. 7 we may expect that other package structures will not show larger differences than the examined one. This will be checked with further experiments in the near future.

7. Acknowledgements

The authors are indebted to E. Kollár and I. Hajas for their help in doing most of the measurements. This work was partially supported by the PROFIT IST-1999-12529 Project of the EU, and by the 2/018/NKFP-2001 INFOTERM Project of the Hungarian Government.

8. References

[1] F.P.Incropera and D.P.DeWitt: Fundamentals of heat and mass transfer, 4th edition, John Wiley and Sons Inc. 1996

[2] P. D. Maycock: “Thermal conductivity of silicon, germanium, III-V compounds and III-V alloys.” *Solid-State Electronics*, V.10, pp. 161-168 (1967)

[3] Christiaens, B. Vandevelde, E. Beyne, R. Mertens, J. Berghmans: "A Generic methodology for Deriving Compact Dynamic Thermal Models, Applied to the PSGA package” IEEE Trans. On Components, Packaging and Manufacturing Technology, Part A Vol 21, No.4 Dec.1998 pp 565-576

[4] J. W. Sofia: “Analysis of thermal transient data with synthetized dynamic models for semi-conductor devices”, *IEEE Trans. on Comp. Pack. & Manuf.* Vol. 18, No.1. pp. 39-47 (1995)

[5] G. Noebauer:” Creating Compact models Using standard spreadsheet software”, Semitherm 2001, San Jose, CA, USA, Proceedings pp 126-134

[6] M. Rencz and V. Székely: Studies on the non-linear effects in dynamic compact model generation of packages, THERMINIC Workshop,1-4 Oct. 2002, Madrid, Spain, pp 10-16

[7] V. Székely and Tran Van Bien: “Fine structure of heat flow path in semiconductor devices: a measurement and identification method”, *Solid-State Electronics*, Vol. 31, pp.1363-1368 (1988)

[8] V. Székely: „THERMODEL: a tool for compact dynamic thermal model generation”, *Microelectronics Journal*, Vol. 29. pp 257-267 (1998)

[9] http://www.micred.com/t3ster.html

[10] V. Székely: “Accurate calculation of device heat dynamics: a special feature of the Trans–Tran circuit analysis program”, *Electronics Letters*, Vol 9, no.6, pp. 132-134 (1973)